THE JOURNAL OF BIOLOGICAL CHEMISTRY
Vol. 276, No. 23, Issue of June 8, pp. 20136–20143, 2001

Printed in U.S.A.

The Bifunctional *Entamoeba histolytica* Alcohol Dehydrogenase 2 (EhADH2) Protein Is Necessary for Amebic Growth and Survival and Requires an Intact C-terminal Domain for Both Alcohol Dehydrogenase and Acetaldehyde Dehydrogenase Activity*

Received for publication, February 12, 2001, and in revised form, March 21, 2001
Published, JBC Papers in Press, March 26, 2001, DOI 10.1074/jbc.M101349200

Avelina Espinosa‡§, Le Yan‡, Zhi Zhang‡, Lynne Foster‡, David Clark¶, Ellen Li‡‖, and Samuel L. Stanley, Jr.‡§**

From the Departments of ‡Medicine, §Molecular Microbiology, and ‖Biochemistry and Molecular Biophysics, Washington University School of Medicine, St. Louis, Missouri 63110 and the ¶Department of Microbiology, Southern Illinois University, Carbondale, Illinois 62901

The intestinal protozoan pathogen *Entamoeba histolytica* lacks mitochondria and derives energy from the fermentation of glucose to ethanol with pyruvate, acetyl enzyme Co-A, and acetaldehyde as intermediates. A key enzyme in this pathway may be the 97-kDa bifunctional *E. histolytica* alcohol dehydrogenase 2 (EhADH2), which possesses both alcohol dehydrogenase (ADH) and acetaldehyde dehydrogenase activity (ALDH). EhADH2 appears to be a fusion protein, with separate N-terminal ALDH and C-terminal ADH domains. Here, we demonstrate that EhADH2 expression is required for *E. histolytica* growth and survival. We find that a mutant EhADH2 enzyme containing the C-terminal 453 amino acids of EhADH2 has ADH activity but lacks ALDH activity. However, a mutant consisting of the N-terminal half of EhADH2 possessed no ADH or ALDH activity. Alteration of a single histidine to arginine in the putative active site of the ADH domain eliminates both ADH and ALDH activity, and this mutant EhADH2 can serve as a dominant negative, eliminating both ADH and ALDH activity when co-expressed with wild-type EhADH2 in *Escherichia coli*. These data indicate that EhADH2 enzyme is required for *E. histolytica* growth and survival and that the C-terminal ADH domain of the enzyme functions as a separate entity. However, ALDH activity requires residues in both the N- and C-terminal halves of the molecule.

The anaerobic intestinal protozoan parasite *Entamoeba histolytica* converts pyruvate to ethanol in its fermentation pathway (1). The last two steps of this pathway are the conversion of acetyl-CoA to acetaldehyde followed by the reduction of acetaldehyde to ethanol (1). *E. histolytica* possesses at least three enzymes with alcohol dehydrogenase (ADH)[1] activity: a NADP-dependent ADH (EhADH1); a 97-kDa NAD(+)-dependent and Fe^{2+}-dependent bifunctional enzyme with both ADH and acetaldehyde dehydrogenase (ALDH) activities (EhADH2, also known as EhADHE); and a 43-kDa NADP-dependent ADH with some sequence homology to class III microbial alcohol dehydrogenases (EhADH3) (2–5). There are at least two enzymes with ALDH activity, the EhADH2 enzyme and a NADP-dependent ALDH, EhALDH1 (2, 5, 6). Given the presence of multiple ADH and ALDH enzymes in *E. histolytica*, an important question is whether any of these enzymes are essential for *E. histolytica* growth and survival and thus potential targets for anti-amebic therapy.

The EhADH2 enzyme is part of a newly described family of multifunctional enzymes found in Gram-negative and Gram-positive bacteria and the intestinal protozoan parasite *Giardia lamblia* (2, 7–12). EhADH2 and other members of the family appear to be composed of separate C-terminal ADH and N-terminal ALDH domains linked together to create a fusion enzyme (8). The EhADH2 enzyme utilizes NAD and Fe^{2+} as co-factors and does not demonstrate homology with the zinc-dependent ADH enzymes (13). Regions of EhADH2 that could be involved in iron binding and NAD binding have been identified, but a requirement for specific residues in enzymatic activity has not been demonstrated (2). The prototype member of the family is the *Escherichia coli* ADHE enzyme, which is required for the anaerobic growth of *E. coli* (8). Both the ADHE enzyme and the native EhADH2 enzyme form protomers that assemble into large helical structures called spirosomes, which are visible by electron microscopy (5, 14, 15). Episomal expression of the amebic *EhADH2* gene in *E. coli* can complement an ADHE mutation, providing a system for rapid evaluation of the activity of EhADH2 mutants and for testing inhibitors of EhADH2 (16).

Here, we describe studies designed to better understand the structure and function of the EhADH2 enzyme. We have used the constitutive and inducible episomal expression of antisense RNA to EhADH2 in amebae specifically to inhibit EhADH2 expression and assess whether EhADH2 is required for amebic growth and survival.

We have analyzed whether EhADH2 is functionally a fusion enzyme with autonomous ADH and ALDH domains by expressing truncated proteins corresponding to the putative ADH and ALDH regions of EhADH2. Finally, we have used site-directed mutagenesis and deletion analyses to identify residues of EhADH2 that are required for both ADH and ALDH activity and a region of the enzyme that may play a role in EhADH2 dimerization and polymerization.

* This work was supported by National Institutes of Health Grants AI37977, AI30084, and DK52574 and U. S. Department of Energy Contract DE-FG02-88ER13941. Presented in part at the XIII Seminar on Amebiasis, Mexico City, 1997. The costs of publication of this article were defrayed in part by the payment of page charges. This article must therefore be hereby marked "*advertisement*" in accordance with 18 U.S.C. Section 1734 solely to indicate this fact.

** Burroughs Wellcome Scholar in Molecular Parasitology. To whom correspondence should be addressed. Tel.: 314-362-107; Fax: 314-362-3525; E-mail: sstanley@im.wustl.edu.

[1] The abbreviations used are: ADH, alcohol dehydrogenase; ALDH, acetaldehyde dehydrogenase; EhADH2, *Entamoeba histolytica* alcohol dehydrogenase 2; PAGE, polyacrylamide gel electrophoresis; PCR, polymerase chain reaction.

MATERIALS AND METHODS

Escherichia coli Strains—Strains DH5α, BL21 (DE3), and SHH31 (Δ*adhE fad*R *met tyr*T) were used for expression of recombinant proteins (16). Cultures were grown in LB broth medium with agitation at 37 °C, and 1.5% Bacto agar (Difco, Sparks, MD) was added for solid media. For anaerobic growth, the transformed strains were grown on solid (1.5% Bacto agar, Difco) or liquid M9 media in anaerobic jars (BBL GasPak™ system, Becton Dickinson, Sparks, MD) with anaerobic system envelopes (BBL GasPak Plus) (16). Indicator strips were used to confirm anaerobic conditions.

EhADH2 Antisense Constructs—To construct the antisense insert for EhADH2, a PCR product was generated from nucleotides −50 to +1312 of the *EhADH2* gene in the antisense orientation using oligonucleotide primers 5′-AATTGCGGCCGCCTAACCCGTTTTTGGATCAG (forward primer) and 5′-ATAGATCTCCTCCATATGATCCACATCCAAG incorporating *Not*I and *Bgl*II restriction sites, respectively. This fragment was then inserted into plasmid pSA8 (17) replacing the antisense *ehcp5* insert to create pZZ1. 1×10^7 *E. histolytica* HM1:1MSS trophozoites in log phase growth were transfected with 100 ng of plasmid pZZ1, pSA8 (antisense construct against *E. histolytica* cysteine proteinase 5), or the parent pNeo-Act plasmid without an insert (17). Selection was performed by adding 10 μg/ml G418 to TYI-S33 media beginning 48 h after transfection and gradually increasing G418 concentration to 50 μg/ml over 2 weeks' time.

The EhADH2 antisense RNA under an inducible expression system was generated by PCR from −50 to +1312 of the EhADH2 sequence as template and synthetic oligonucleotide primers 5′-GAGGATCCTAACCCGTTTTTGGATCAG (forward primer) and 5′-GAGGTACCTCCATATGATCCACATCCAAG incorporating *Bam*HI and *Kpn*I restriction sites, respectively. The PCR product was ligated into pEhHYG-tetR-O-CAT (graciously provided by Egbert Tannich, Bernhard Nocht Institute, Hamburg, Germany) (18) using the *Kpn*I and *Bam*HI restriction sites to obtain plasmid pEhHYG-tetR-O-EhADH2 (Fig. 2). 1×10^7 *E. histolytica* trophozoites were transfected with 100 ng of plasmid pEhHYG-tetR-O-EhADH2 or pEhHYG-tetR-O-CAT as described previously (18). Hygromycin selection (10 μg/ml) was initiated 48 h after transfection.

Assays of EhADH2 Expression and E. histolytica Growth—To assay *E. histolytica* trophozoite growth during expression of the antisense RNA to EhADH2, starting cultures of 5×10^3 trophozoite transfected with pZZ1, pSA8, or pNeo-Act were grown under 50 μg/ml G418 selection and counted at 48 and 72 h. Results were averaged from three replicate tubes and three separate experiments. For studies of the inducible expression of the EhADH2 antisense RNA, separate cultures of 5×10^3 *E. histolytica* pEhHYG-tetR-O-EhADH2 (anti-EhADH2) or pEhHYG-tetR-O-CAT (p-CAT) transfected trophozoites were grown for 48 h and treated with 1 μg/ml tetracycline. After tetracycline induction, cultures were grown for 48 h. *E. histolytica* trophozoites were harvested by chilling culture tubes on ice for 10 min and centrifuging them at $430 \times g$ for 5 min. The resulting pellets were resuspended in 1 ml of BYI-S-33 medium and the trophozoites counted with a hemocytometer. EhADH2 expression in *E. histolytica* trophozoites transfected with pZZ, pSA8, pNeo-Act, pEhHYG-tetR-O-EhADH2, or pEhHYG-tetR-O-CAT was assessed by immunoblotting using a 1:10000 dilution of rabbit antiserum raised to a recombinant 6His-EhADH2 fusion protein on SDS-PAGE-separated lysates obtained from 1×10^6 trophozoites (16). Scanning densitometry of autoradiographs was performed using a DuoScan scanner from Agfa (Ridgeway Park, NJ).

Assessment of ADH and ALDH Activity in E. histolytica Transfected with EhADH2 Antisense Constructs—Approximately 1×10^8 ameba trophozoites from each of the transfectants described above (pZZ, pEhHYG-tetR-O-EhADH2, pSA8, and pEhHYG-tetR-O-CAT), grown under conditions to maximize antisense RNA expression, were harvested by chilling on ice for 10 min and centrifuged at $430 \times g$ at 4 °C for 5 min. The pellet was resuspended in 800 μl of lysis buffer B (20 mM Tris-HCl, pH 6.5, 2 μM leupeptin, 5 mM *N*-ethylmaleimide, 2 mM phenylmethylsulfonyl fluoride, 2 mM benzamidine, and 5 mM E-64), freeze-thawed five times in ethanol/CO_2, and centrifuged at $150{,}000 \times g$ at 4 °C for 40 min. The supernatant was kept on ice and the activity assays performed immediately. Protein concentrations were calculated using the Bradford method. ADH activity of the amebic lysates (or bacterial lysates from subsequent experiments) was determined by measuring the decrease in absorbance at 340 nm following the oxidation of NADH to NAD. The standard assay was performed in the presence of 6 mM dithiothreitol, 5 mM $MgSO_4$, 0.1 mM Fe $(NH_4)_2(SO_4)_2$, 0.2 mM NADH, 0.5 mM acetaldehyde, and 0.1 Tris-HCl buffer, pH 6.5 (16). The ALDH activity was performed in the same buffer, replacing the acetaldehyde with 0.2 mM acetyl-CoA. One unit of enzyme activity was defined as that which consumes 1 μmol of NADH or NAD^+/min. Values are expressed as the means of at least three independent experiments. For the determination of K_m values for the EhADH2 and EhADH2-(417–870) proteins, 5 μg of purified recombinant protein was used in each assay. K_m determinations for alcohol substrates with EhADH2 and EhADH2-(417–870) were made with the spectrophotometric assay in the reverse reaction, using 1 mM NAD^+ rather than NADH as previously described (16). K_m values were calculated using Lineweaver-Burk plots.

Construction of the pEhADH2-(1–532) and pEhADH2-(417–870) Expression Vectors—The T7 promoter-based vector pET23a (Novagen, Madison, WI) was used for *E. coli* expression of recombinant proteins comprising the N-terminal domain (EhADH2-(1–532)) and the C-terminal domain (EhADH2-(417–870)) of EhADH2 (Fig. 1). Nucleotides encoding EhADH2-(1–532) were obtained by PCR from the pET3a/EhADH2 construct (16). The sequences flanking the nucleotides encoding EhADH2-(1–532) were modified by the incorporation of a stop codon and a *Bam*HI site at position 1598 of the EhADH2 DNA sequence. The fragment containing EhADH2-(1–532) was then ligated into a *Nde*I- and *Bam*HI-digested pet23a vector to generate plasmid pEhADH2-(1–532). Nucleotides encoding EhADH2-(417–870) were also obtained by PCR from the pET3a/EhADH2 construct. The sequences flanking regions encoding EhADH2-(417–870) were modified by the incorporation of a *Bam*HI site next to the termination codon TAA at position 2612 at the 3′ end of EhADH2 and a *Nhe*I site with an initiating codon at position 1251 of the EhADH2 DNA sequence (2). The fragment containing EhADH2-(417–870) was then ligated into *Nhe*I- and *Bam*HI-digested pET23a vector creating plasmid pEhADH2-(417–870).

Site-directed and Deletion Mutagenesis of EhADH2—The recombinant pET3a/EhADH2 vector was used to generate site-directed and deletion mutants using the QuickChange™ site-directed mutagenesis kit (Stratagene, La Jolla, CA). In separate constructs, the histidines at position 88, 730, 734, or 744 of recombinant EhADH2 were replaced by arginine, and the histidine at position 754 was replaced by arginine or glutamine, generating mutants EhADH2(H88R), EhADH2(H730R), EhADH2(H734R), EhADH2(H744R), EhADH2(H754R), and EhADH2-(H754Q). All changes were confirmed by sequence analysis of each plasmid. These replacements are marked in Fig. 1. To generate a C-terminal deletion, the hydrophobic stretch of 17 amino acids at the end of EhADH2 was deleted using a modified PCR reaction (19).

Expression of Truncated and Mutant Versions of EhADH2—Plasmids carrying the N- and C-terminal domains of EhADH2 and plasmids carrying mutant EhADH2 were expressed separately in BL21 (DE3) by standard procedures. For each strain, a single colony was grown overnight in 1-liter cultures under aerobic conditions. Cells were collected by centrifugation at $1{,}500 \times g$ for 30 min and resuspended in 20 mM Tris-HCl (pH 6.5). Samples were disrupted by sonication and sedimented by centrifugation at $13{,}000 \times g$ for 30 min at 4 °C. The supernatant was filtered with a 0.22-micron pore unit, and protein concentration was determined by the Bradford assay (Bio-Rad). Each sample (5 μg) was analyzed by SDS-PAGE analysis to detect expression of the altered EhADH2 protein. Western blot analysis was performed using a 1:10,000 dilution of rabbit antiserum raised to a recombinant 6His-EhADH2 fusion protein as described previously (16). For functional studies, SHH31 (Δ*adhE*) was transformed separately with plasmids carrying the altered version of EhADH2. Expression of the mutant proteins by SHH31 (Δ*adhE*) under aerobic conditions was confirmed by SDS-PAGE and immunoblot analyses. Bacterial lysates from each transformed strain were tested for ADH and ALDH activities as described above. To test for the ability of a mutant EhADH2 protein to complement SHH31 for anaerobic growth, individual colonies from the transformed strain were grown in 14 ml of M9 liquid or on M9 agar for 24, 48, and 72 h under anaerobic conditions (16). Growth was measured spectrophotometrically by absorbance at 600 nm or by counting colonies on agar.

Co-expression of EhADH2(H754R) and EhADH2 in SHH31—The sequence encoding EhADH2(H754R) was inserted in plasmid pET29b, which contains a selectable marker for kanamycin resistance (Novagen). The pEhADH2 plasmid contains an ampicillin selection marker. Strain SHH31 (Δ*adhE*) was co-transformed by electroporation with 2 μg (each) of pEhADH2 (recombinant wild type) and pEhADH2(H754R). Isolated colonies were selected from clones grown in the presence of both kanamycin and ampicillin. Single colonies were grown overnight in 1 liter of LB broth medium under double antibiotic selection. Plasmids pEhADH2 (positive control), pEhADH2(H754R), pET3a, and pET29b (negative controls) were expressed separately. Bacterial lysates were obtained and tested for expression of recombinant EhADH2 proteins, anaerobic growth, and ADH/ALDH activities as described above.

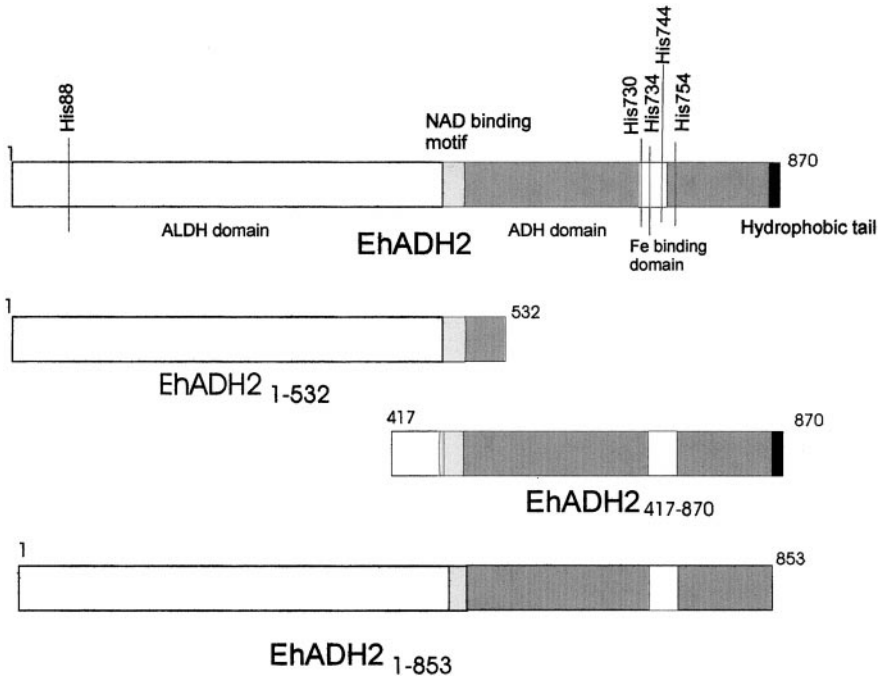

FIG. 1. **Schematic diagram of EhADH2 and EhADH2 mutant proteins.** The locations of the putative ADH and ALDH domains, the NAD-binding motif, iron-binding domain, and hydrophobic tail are indicated. The histidines replaced by site-directed mutagenesis are also marked. The composition of the three main deletion mutants, EhADH2-(1–532), EhADH2-(417–870), and EhADH2-(1–853), is also shown.

Retention of pEhADH2 within SHH31 was shown by reselection of the doubly transfected SHH31 with ampicillin alone, followed by assessment of growth under anaerobic conditions.

Sizing Exclusion Analysis—Sepharose CL-6B (Sigma) was used to size engineered EhADH2 proteins. A single colony of each transformed strain was grown overnight under aerobic conditions. Bacterial cells were pelleted by centrifugation, resuspended in lysis buffer, disrupted by French press, and sedimented by centrifugation as described above. Filtered samples were separated over a Sepharose CL-6B column equilibrated with 20 mM Tris-HCl (pH 6.5). Fractions were collected and measured spectrophotometrically at 280 nm. Each protein was sized by comparison with molecular weight standards (Sigma). EhADH2 proteins in samples were identified by immunoblotting of SDS-PAGE separated fractions.

Spirosome Detection by Electron Microscopy—For studies of spirosome formation by EhADH2 and its altered derivatives, 100 ng of protein from cell lysates were absorbed to a 200-mesh nickel Formvar- and carbon-coated grids, negatively stained with 0.05% uranyl acetate, and photographed using a Zeiss 902 electron microscope (15).

RESULTS

Episomal Expression of an Antisense RNA to the EhADH2 Gene Inhibits E. histolytica Growth—To analyze the role of EhADH2 enzymatic activity in the growth and survival of *E. histolytica*, we transformed amebae with the plasmid pZZ1, constitutively expressing an antisense EhADH2 transcript. Amebic lysates derived from pZZ1-transfected trophozoites had 30% of the ADH activity of lysates derived from equivalent numbers of wild type HM1:IMSS trophozoites or trophozoites transformed with plasmid pSA8 (which contains an antisense transcript to the *E. histolytica* cysteine proteinase 5 gene) (Table I) (17). Using immunoblotting with antiserum raised against EhADH2, we found that EhADH2 was present in lower amounts (83% reduction by scanning densitometry of the autoradiograph bands) in SDS-PAGE-separated lysates from pZZ1-transfected *E. histolytica* compared with lysates from pSA8-transfected *E. histolytica* (Fig. 2). In contrast, expression of the serine-rich *E. histolytica* protein (SREHP) (measured by immunoblotting with anti-SREHP monoclonal antibody) did not differ between pZZ1 and wild type trophozoites (data not shown). To look at the effects of reduced EhADH2 synthesis, we measured the growth of pZZ1 transfected *E. histolytica* trophozoites by inoculating a culture tube with 5×10^3 *E. histolytica* trophozoites and then counting viable trophozoites 48 and 72 h after inoculation. We used pSA8-transfected trophozoites as a control for both G418 selection and possible nonspecific effects of antisense expression on amebic growth. As shown in Fig. 3*A*, both sets of transgenic *E. histolytica* trophozoites under antibiotic selection with G418 have reduced growth compared with wild type trophozoites. However, amebic trophozoites transfected with the pZZ1 plasmid show significantly reduced growth compared with trophozoites transfected with pSA8.

We confirmed that the reduced growth seen in these trophozoites was caused by expression of the antisense EhADH2 RNA by inducing expression of the antisense RNA in log phase *E. histolytica* trophozoites. The pEhHYG-tetR-O-EhADH2 plasmid was used to transform *E. histolytica* HM1:IMSS trophozoites, while HM1:IMSS trophozoites transformed with the pEhHYG-tetR-O-CAT construct served as controls. Transformants were selected for growth in 10 μg/ml hygromycin, and both sets

TABLE I
Constitutive expression of an antisense RNA to EhADH2 significantly reduces NAD-dependent ADH and ALDH activities in E. histolytica trophozoites

Lysates were obtained from 10^6 amebae transfected with either pSA8 (expressing an antisense RNA for *Ehcp5*) or pZZ1 (expressing the antisense RNA for *Ehadh2*). Results are expressed as the mean ± standard error of the mean from three separate experiments.

Plasmid	Antisense to	ADH activity	ALDH activity
		milliunits/mg	
pSA8	*E. histolytica* cysteine proteinase 5 gene (*Ehcp5*)	185 ± 15	78 ± 13
pZZ1	*Ehadh2*	56 ± 11	23 ± 9

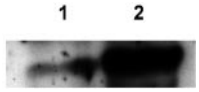

FIG. 2. **Lysates from *E. histolytica* trophozoites transfected with pZZ1 (antisense RNA to *Ehadh2*) contain a reduced amount of EhADH2.** SDS-PAGE-separated lysates from 10^6 *E. histolytica* HM1:IMSS trophozoites transfected with pZZ1 (*lane 1*) or wild-type HM1:IMSS (*lane 2*) were subjected to immunoblotting with anti-EhADH2 antiserum. The intensity of the bands at 97 kDa (EhADH2) is compared.

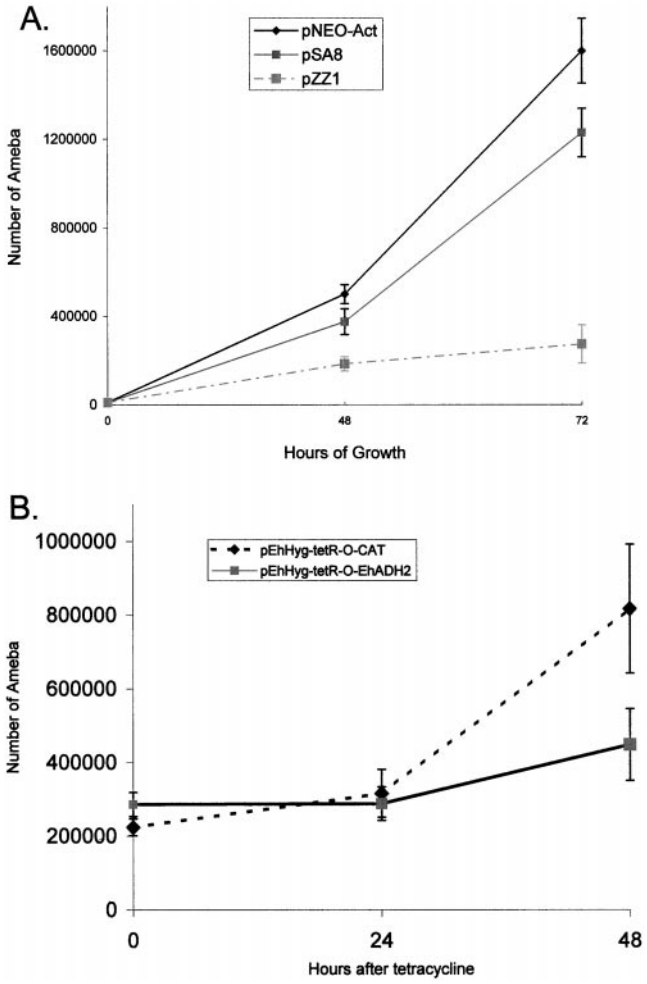

FIG. 3. **Antisense inhibition of EhADH2 synthesis reduces *E. histolytica* growth.** *Panel A*, separate starting cultures of 5×10^3 trophozoites carrying either pSA8 or pZZ1 or the control plasmid pNeo-Act were grown under G418 selection and counted at 48 and 72 h ($n = 6$ for each group). There was a statistically significant ($p < 0.001$) difference in the number of pZZ1-transfected trophozoites at 72 h. *Panel B*, 48-h cultures of *E. histolytica* trophozoites carrying pEhHYG-tetR-O-CAT or pEhHYG-tetR-O-EhADH2 were treated with tetracycline and their growth monitored over 24 and 48 h. The addition of tetracycline significantly inhibited growth ($p < 0.001$) in the pEhHYG-tetR-O-EhADH2-transfected amebae at 48 h.

of transformants showed similar growth curves under continuous hygromycin selection (data not shown). We then grew equivalent starting cultures of trophozoites carrying pEhHYG-tetR-O-EhADH2 and trophozoites carrying pEhHYG-tetR-O-CAT in the added presence of 1 μg/ml tetracycline, and the number of trophozoites was counted at 24 and 48 h following the addition of tetracycline. As shown in Fig. 3*B*, the addition of tetracycline caused a significant inhibition of the growth of pEhHYG-tetR-O-EhADH2-transformed amebae at 48 h but did not alter the growth of pEhHYG-tetR-O-CAT-transformed trophozoites. To establish that this difference in growth was due to inhibition of EhADH2 synthesis, we measured ADH and ALDH activity in the lysates of 10^6 pEhHYG-tetR-O-EhADH2-transfected or pEhHYG-tetR-O-CAT-transfected trophozoites that had been cultured for 48 h in the presence of tetracycline. There was a 70% reduction in ADH activity and a 66% reduction in ALDH activity in pEhHYG-tetR-O-EhADH2-transfected trophozoites compared with pEhHYG-tetR-O-CAT-transfected trophozoites at 48 h after tetracycline addition (Table II).

TABLE II
Induced expression of an antisense RNA to EhADH2 significantly reduces NAD-dependent ADH and ALDH activities in E. histolytica trophozoites

ADH and ALDH activities were measured in the lysates from 10^6 amebae transfected with either the vector alone (pEhHYG-tetR-O-CAT) or with the plasmid encoding the *Ehadh2* antisense sequence (pEhHYG-tetR-O-EhADH2). For values after tetracycline induction, *E. histolytica* trophozoites were isolated 48 h after growth in 1 μg/ml tetracycline.

Plasmid	ADH activities		ALDH activities	
Tetracycline	+	−	+	−
	milliunits/mg			
pEhHYG-tetR-O-CAT	210 ± 21	203 ± 18	113 ± 13	117 ± 19
pEhHYG-tetR-O-EhADH2	83 ± 12	191 ± 23	37 ± 8	122 ± 22

of the Enzyme—The C-terminal 400 amino acids of EhADH2 show significant homology with class III microbial ADH from organisms such as *Clostridium acetobutylicum* and *Zymomonas mobilis (2)*. If the EhADH2 enzyme is truly a fusion enzyme, with distinct ADH and ALDH enzymes linked to form a single peptide, then expression of the individual domains should produce separate functional ADH and ALDH enzymes. To test this hypothesis, we first expressed nucleotides 1251–2612 of EhADH2 in *E. coli* BL21 and SHH31 to generate a truncated protein containing the entire ADH domain (EhADH2-(417–870)). Expression of EhADH2-(417–870) was confirmed by immunoblotting using polyclonal antiserum to the full-length EhADH2 protein (data not shown). Assays of ADH activity on *E. coli* SHH31 lysates and on purified EhADH-(417–870) demonstrated that the truncated protein retained ADH activity similar in magnitude to that seen with the full-length EhADH2 enzyme (Table III). EhADH2-(417–870) did not possess ALDH activity (Table III). The K_m values for EhADH2-(417–870) and EhADH2 for the substrates ethanol, acetaldehyde, acetyl-CoA, propanol, and isopropanol were determined (Table IV). The K_m values for EhADH2-(417–870) were lower than those obtained for EhADH2 for all substrates tested, and EhADH2-(417–870) was able to utilize isopropanol as a substrate. Gel filtration analysis revealed that EhADH2-(417–870) (predicted molecular mass, 49 kDa) migrated in a fraction consistent with a molecular mass of ~200 kDa (Fig. 4). Electron microscopic analysis of either the >2000-kDa fraction or the 200-kDa fraction did not reveal spirosome formation (data not shown). For comparison, the full-length EhADH2 enzyme (97.4 kDa) is found in the > 2000-kDa fraction (Fig. 4), where it forms spirosomes (Fig. 5), or at 200 kDa consistent with dimer formation (Fig. 4) (16). Episomal expression of EhADH2-(417–870) could not rescue the ability of *E. coli* SHH31 to grow under anaerobic conditions (Fig. 6).

The ALDH Activity of EhADH2 Requires Residues in the C-terminal Half of EhADH2—The N-terminal ALDH domain of EhADH2 has positional identities (32%) with the CoA- and NADP-dependent succinate semialdehyde dehydrogenase of *Clostridium kluyveri* and retains a number of residues known to be required for ALDH activity (20–22). To determine whether the N-terminal region of EhADH2 encoded a functional ALDH enzyme, we expressed nucleotides 1–1566 of EhADH2 in *E. coli* BL21 (DE3) and *E. coli* SHH31 (Δ*adhE*) generating a truncated protein (EhADH2-(1–522)) containing the entire ALDH domain plus a potential NAD binding site (Fig. 1). Expression of the $EhADH2_{1–522}$ protein (predicted molecular mass, 58 kDa) was confirmed by immunoblotting using polyclonal antiserum to the full-length EhADH2 protein (data not shown). Assays on *E. coli* SHH31 lysates and purified EhADH2-(1–522) protein showed no ALDH or ADH activity (Table III). In gel filtration, EhADH2-(1–522) migrated in a

TABLE III

NAD-dependent ADH and ALDH dehydrogenase activities measured from partially purified bacterial lysates of E. coli SHH31 expressing either wild type recombinant EhADH2 enzyme, one of the indicated EhADH2 mutants, or plasmid without an insert

ND, no activity (<1 milliunit/mg) detected).

EhADH2 version	ADH activity	ALDH activity
	milliunits/mg	
(None) plasmid pET3a	ND	ND
EhADH2 wild type	500 ± 43	220 ± 32
EhADH2-(417–870)	808 ± 313	ND
EhADH2-(1–532)	ND	ND
EhADH2-(1–853)	ND	ND
(None) pET3a and pET39b	ND	ND
EhADH2(H88R)	423 ± 110	198 ± 72
EhADH2(H730R)	ND	ND
EhADH2(H734R)	149 ± 24	ND
EhADH2(H744R)	ND	ND
EhADH2(H754R)	ND	ND
EhADH2(H754Q)	ND	ND
EhADH2 and EhADH2(H754R)	ND	ND
EhADH2 (after curing EhADH2(H754R))	537 ± 54	350 ± 117

TABLE IV

K_m values for different substrates for EhADH2$_{417–870}$ compared with the wild type EhADH2 enzyme

25 μg of purified enzyme was used for each assay. ND, no activity detected.

Reactions	K_m for EhADH2	K_m for EhADH2$_{417–870}$
	mM	
Acetaldehyde + NADH	0.21	0.083
	0.32	0.028
Acetyl-CoA + NADH	0.028	ND
	0.1	ND
Ethanol + NAD^+	50	0.079
	0.2	0.062
l-Propanol + NAD^+	34	0.081
	0.19	0.073
Isopropanol + NAD^+	ND	0.077
	ND	0.065

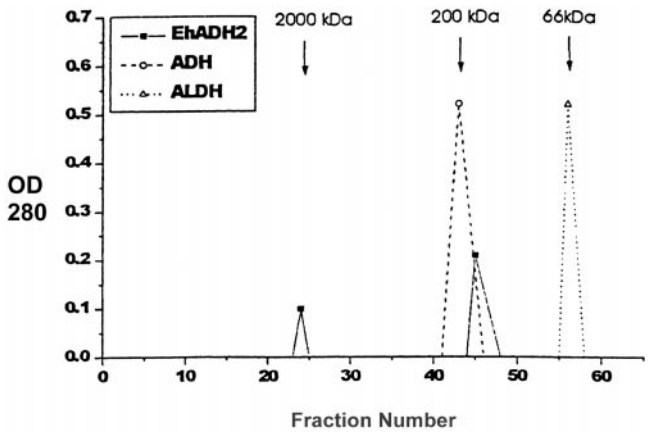

FIG. 4. **Size analysis of purified fractions of the full-length EhADH2 and the truncated EhADH2-(1–532) (ALDH) and EhADH2-(417–870) (ADH) peptides.** The *ordinate* represents protein concentration in at $A_{280\ nm}$. The EhADH2 enzyme was detected at >2000 kDa as well as at 200 kDa. The ADH domain protein migrates at ~200 kDa, whereas the ALDH domain migrates at 66 kDa, consistent with a monomer. The *arrows* show the fraction where the indicated molecular mass standards elute.

fraction consistent with a molecular mass of ~66 kDa and was not detected in the >2000-kDa fraction or the 200-kDa fraction (Fig. 4), and electron microscope analysis of the >2000-kDa fraction did not show spirosomes (data not shown). The episomal expression of EhADH2-(1–522) could not rescue the ability of *E. coli* SHH31 (Δ*adhE*) to grow under anaerobic conditions (Fig. 6). To determine whether the lack of ALDH activity of

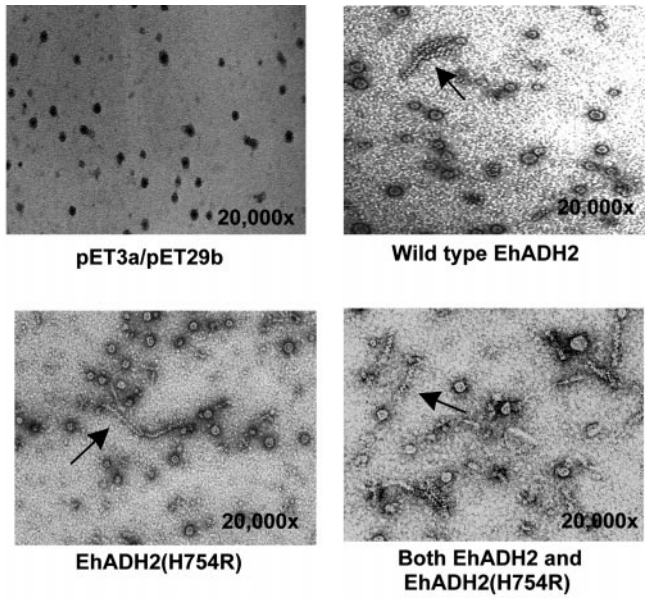

FIG. 5. **Spirosome formation in partially purified lysates from bacteria expressing either EhADH2 or EhADH2(H754R) or both EhADH2 and EhADH2(H754R).** Electron micrographs show spirosomes (*arrows*) in these fractions. Lysates from bacteria carrying both vectors without inserts did not show spirosome formation (*pET3a/pET29b*).

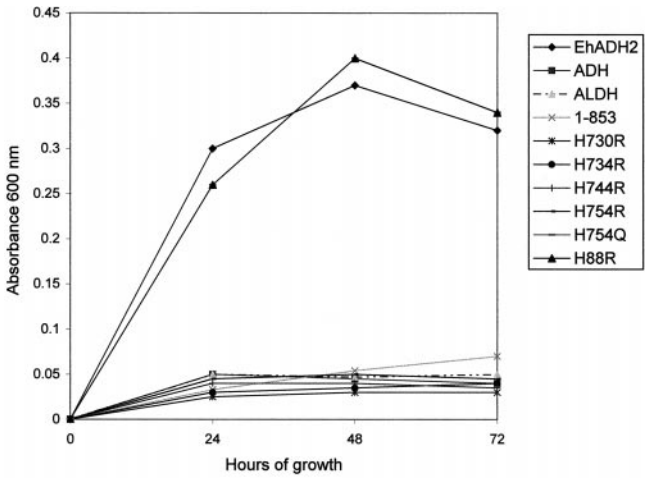

FIG. 6. **Rescue of anaerobic growth of *E. coli* SHH31 (Δ*adhE*) by wild type EhADH2 and mutant EhADH2 enzymes.** *E. coli* SHH31 (Δ*adhE*) transformed with plasmids encoding full-length EhADH2, EhADH2-(1–532) (*ALDH*), EhADH2-(417–870) (*ADH*), EhADH2-(1–853) (*1–853*), EhADH2(H88R) (*H88R*), EhADH2(H730R) (*H730R*), EhADH2(H734R) (*H734R*), EhADH2(H744R) (*H744R*), EhADH2(H754R) (*H754R*), or EhADH2(H754Q) (*H754Q*) was grown in liquid medium under anaerobic conditions, and $A_{600\ nm}$ was measured at 0, 24, 48, and 72 h after inoculation. Only full-length EhADH2 and the EhADH2(H88R) mutant could restore growth under anaerobic conditions.

EhADH2-(1–522) was due to a lack of additional C-terminal residues including the putative iron-binding domain, we generated a deletion mutant lacking only the C-terminal 17 amino acids of EhADH2 (EhADH2-(1–853)) (Fig. 1). This mutant enzyme lacked both ADH and ALDH activity (Table III), and under gel filtration it migrated primarily in the >2000-kDa fraction (data not shown). However, electron microscopic analysis of that fraction failed to reveal spirosomes (data not shown). Episomal expression of EhADH2-(1–853) could not rescue the ability of *E. coli* SHH31 to grow under anaerobic conditions (Fig. 6).

Conserved Histidines in the ADH Domain of EhADH2 Are

Required for Both ADH and ALDH Activity—EhADH2 possesses a histidine at position 754 that is similar in location to a histidine implicated in the catalytic mechanism of the *Z. mobilis* ADH(II) enzyme (23). Replacement of His^{754} with either Gln or Arg completely eliminated both the ADH and ALDH activity of recombinant EhADH2 (Table III). In gel filtration analysis, EhADH2(H754R) was found in the 200-kDa and >2000-kDa fraction, and spirosomes were found in the >2000-kDa fraction (Fig. 5). Episomal expression of the mutant EhADH2(H754R) enzyme could not restore the ability of *E. coli* SHH31 to grow under anaerobic conditions (Fig. 6). Another set of highly conserved histidine residues, $GMDH^{730}SMAH^{734}KVGAAFHLPH^{744}G$, is found in the putative iron-binding domain of the EhADH2 enzyme. To determine whether these residues are required for EhADH2 activity, we generated mutant EhADH2 enzymes with selected histidines replaced by arginine: EhADH2(H730R), EhADH2(H734R), EhADH2(H744R). In addition, we made EhADH2(H88R) because this histidine is not predicted to be within the active sites of either the ADH or ALDH domains. Lysates from *E. coli* expressing EhADH2(H730R) and EhADH2(H744R) lacked both ADH and ALDH activity, whereas EhADH2(H734R) possessed reduced ADH activity. EhADH2(H88R) was identical to wild type EhADH2 in both ADH and ALDH activity (Table III). Among the mutant EhADH2 enzymes, only EhADH2(H88R) could rescue the anaerobic growth of *E. coli* SHH31 ΔadhE (Fig. 6).

Spirosome-forming EhADH2(H754R) Functions as a Dominant Negative Mutant—It has been proposed that EhADH2 and the *E. coli* adhE enzyme must form dimers or multimers (spirosomes) for activity (2, 5, 14); this suggests that the episomal expression of a nonfunctional EhADH2 enzyme capable of forming spirosomes could serve as a dominant negative mutant by pairing and oligomerizing with the native enzyme. We found that the nonfunctional mutant EhADH2(H754R) mutant was capable of forming spirosomes (Fig. 5) but did not possess EhADH2 activity. We co-transformed *E. coli* SHH31 with EhADH2 on plasmid pET3a/EhADH2 *amp*R and pEhADH2(H754R) *kan*R. *E. coli* expressing both antibiotic resistance plasmids were obtained by selection with kanamycin and ampicillin under aerobic conditions, and spirosome formation was assessed. As shown in Fig. 5, spirosomes could be detected in partially purified lysates obtained from *E. coli* SHH31 transformed with either pEhADH2 or pEhADH2(H754R) or with both plasmids. No spirosomes were seen in *E. coli* co-transformed with both parent plasmids (pET3a and pET29b). Subsequently, the double transformants were screened for the ability to grow under anaerobic conditions. *E. coli* expressing both EhADH2 and EhADH2(H754R) failed to grow under anaerobic conditions in either liquid (Fig. 7) or solid media (data not shown). Curing of SHH31 doubly transformed with pEhADH2 and pEhADH2(H754R) of the pEhADH2(H754R) plasmid by removing kanamycin selection restored the ability of *E. coli* SHH31 to grow under anaerobic conditions (Fig. 7).

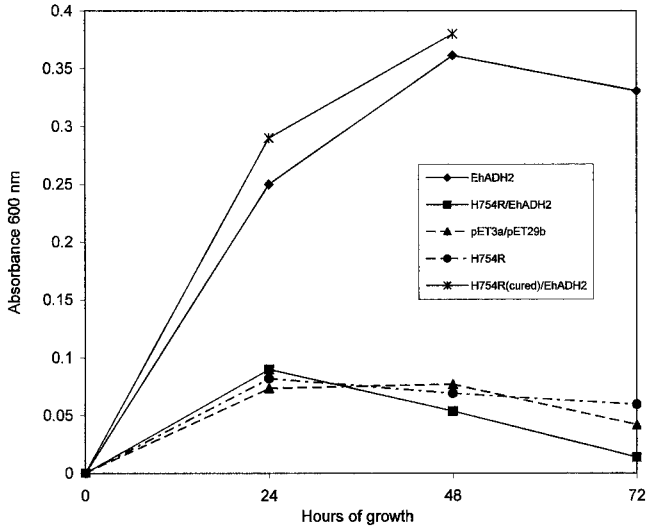

FIG. 7. **Co-expression of EhADH2(H754R) blocks the ability of wild type EhADH2 to rescue the anaerobic growth of *E. coli* SHH31 (Δ*adhE*).** Anaerobic growth of SHH31 transformed with plasmids expressing either EhADH2 or EhADH2(H754R) (*H754R*), both EhADH2 and EhADH2(H754R) (*H754R/EhADH2*), or both plasmids without inserts (*pET3a/pET29b*) is shown. *E. coli* SHH31 (Δ*adhE*) transformed with both EhADH2 and EhADH2(H754R) was subsequently grown without kanamycin selection to cure it of the pEhADH2(H754R) plasmid (*H754R(cured)/EhADH2*). Only *E. coli* SHH31 (Δ*adhE*), transformed with a plasmid expressing EhADH2, or the doubly transfected *E. coli* SHH31 (Δ*adhE*), cured of the plasmid expressing EhADH2(H754R), could grow under anaerobic conditions.

DISCUSSION

The glycolytic pathway for the anaerobic protozoan parasite *E. histolytica* was first described by Reeves (1, 24) more than two decades ago. A number of the *E. histolytica* metabolic enzymes appear to be derived from ancestral prokaryotic enzymes and are significantly different from eukaryotic homologues (7). The EhADH2 enzyme (also referred to as EhADHE) is a 97-kDa NAD- and Fe^{2+}-dependent bifunctional enzyme with both ADH and ALDH activities (2,5). This enzyme does not have a homologue in man. Its proposed function in *E. histolytica* is to catalyze the final two steps in the amebic glycolytic pathway, which are the conversion of acetyl-CoA to acetaldehyde and the reduction of acetaldehyde to ethanol. However, *E. histolytica* possesses other ADH and ALDH enzymes that could potentially serve a similar function. There are two structurally distinct NADP-dependent ADH molecules, EhADH1 and EhADH3 (3, 4). There is also a NADP-dependent ALDH, EhALDH1 (6). Despite the presence of these other enzymes, there is experimental evidence that the EhADH2 enzyme is required for both the conversion of acetyl-CoA to acetaldehyde and acetaldehyde to ethanol in *E. histolytica*. The conversion of acetaldehyde to ethanol is NADH- rather than NADPH-dependent (1). The EhADH1 enzyme, which is NADP-dependent, shows a marked preference for branched chain alcohols, whereas EhADH2 prefers ethanol as a substrate (2,3). In addition, the EhALDH1 enzyme does not utilize acetyl Co-A as a substrate, suggesting that EhADH2 may be solely responsible for the conversion of acetyl-CoA to acetaldehyde (6).

To test directly whether EhADH2 is necessary for *E. histolytica* growth and survival, we specifically decreased the expression of EhADH2 through the episomal expression of an antisense RNA to the *EhADH2* gene. Targeted disruption of amebic genes has not yet been achieved; however, episomal expression of antisense RNA has been used specifically to inhibit the expression of *E. histolytica* genes. This approach does not result in complete inhibition of protein expression, but it has reduced the levels of the target protein by 70–90% (17). In our hands, constitutive expression of an antisense RNA to EhADH2 reduced NAD-dependent ADH activity by 60–70%. This was accompanied by a marked decrease in amebic growth and viability, compared with either amebae carrying the vector lacking the antisense insert or amebae expressing an antisense construct to the amebic cysteine proteinase gene. Similar results were seen using an inducible expression system in which *E. histolytica* growth was significantly inhibited with induction of the antisense RNA. These results are very different from the data seen with antisense inhibition of expression of the *E. histolytica* cysteine proteinase 5 gene, the *E. histolytica* amebapore A gene, or the light chain of the galactose binding lectin,

where expression of antisense RNA did not significantly inhibit trophozoite growth or survival (17, 25, 26). These data suggest that EhADH2 is responsible for most, if not all, of the NAD-dependent ADH and ALDH activity in *E. histolytica* and that the expression of EhADH2 is necessary for growth and survival of amebic trophozoites under anaerobic conditions. A potential problem with the use of antisense RNA is whether the inhibition of protein expression is limited to the targeted molecule. We found no changes in the levels of amebic cysteine proteinase activity or expression of the amebic serine-rich protein in amebae carrying the EhADH2 antisense construct but cannot absolutely exclude the possibility that the expression of other proteins could have been affected.

Enzymes homologous to EhADH2 have been found in Gram-positive and Gram-negative bacteria and in the intestinal protozoan parasite *G. lamblia* (7, 8–12, 20). Despite the potential clinical importance of this new family of enzymes, little is known about their structure and catalytic mechanisms. Based on homology with separate ADH and ALDH enzymes, members of this family appear to be fusion enzymes, with a discrete C-terminal ADH domain and N-terminal ALDH domain (8). The ADH domain of EhADH2 displays limited homology with members of the small family of class III microbial ADH enzymes, the prototype of which is the Fe^{2+}-dependent ADH(II) enzyme from the anaerobic bacterium *Z. mobilis* (2, 27, 28). We found that the C-terminal 453 amino acids of EhADH2 contained all of the residues necessary for NAD-dependent ADH activity, consistent with the fusion enzyme hypothesis. These data are similar to those found in studies of the *E. coli* AdhE enzyme, in which ADH activity could be localized to a peptide containing ~300 amino acids in the C-terminal region (14). Based on its migration under gel filtration, the mutant EhADH2-(417–870) enzyme appeared to form tetramers rather than the dimers or spirosomes seen with the full-length EhADH2 enzyme. Interestingly, other class III iron-dependent ADH enzymes, including ADHII of *Z. mobilis* and *Bacillus stearothermophilus* RS93, also form homotetramers (27, 29). There were some significant differences in K_m values for the mutant EhADH2-(417–870) enzyme compared with the full-length recombinant EhADH2, and the mutant enzyme, unlike full-length EhADH2 could utilize the branched chain alcohol isopropanol as a substrate. These data indicate that removal of the N-terminal half of the enzyme results in conformational changes that alter the substrate binding pocket in the EhADH2-(417–870) mutant enzyme. However, acetyl Co-A was not a substrate for the ADH domain mutant, consistent with the primary structure of EhADH2 in which residues that could be involved in acetyl Co-A binding are found within the N-terminal half of EhADH2 (2).

Alignment of the N-terminal sequences of members of the ADHE family, including EhADH2, with consensus ALDH sequences shows the conservation of a number of key residues in the catalytic site[2] (2, 22). These include a potential catalytic cysteine at Cys^{252}, a conserved glutamate involved in proton binding at position 350, and a conserved asparagine at position 121 that may be involved in hydrogen bonding to the nicotinamide ring of NAD (21, 22). The EhADH2 enzyme also possesses a classic G*X*G*XX*G NAD binding fingerprint, but it is located at the junction of the putative ALDH and ADH domains (2, 30). A second motif that resembles an NAD-binding domain (GVGAG) is present in the ALDH region, and these residues could play a role in binding the adenine residue of CoA. Thus, the ALDH domain of *E. histolytica* EhADH2 appears to contain the key catalytic residues necessary for ALDH activity and, possibly, appropriate motifs for NADH and acetyl-CoA binding. Despite these homologies, we found that a truncated protein containing the N-terminal 522 amino acids of EhADH2 did not possess either ADH or ALDH activity. One possible explanation for our findings is that the lack of the iron-binding domain within the EhADH2-(1–522) mutant renders it inactive. However, we also found that the deletion of only 17 amino acids in the C terminus of the EhADH2 (which left the putative iron-binding domain intact) abrogated both ADH and ALDH activity. This mutant enzyme failed to form dimers or spirosomes, suggesting that residues in the C terminus may be necessary for EhADH2 dimer and spirosome formation and thus indirectly for both ADH and ALDH activity.

By comparing the primary structure of the C-terminal domain of EhADH2 with the ADHII of *Z. mobilis*, we were able to identify EhADH2 residues that could play a role in the ADH activity of the enzyme. The ADH domain of members of the ADHE family and the *Z. mobilis* ADH(II) enzyme contains the sequence G*XX*H*XX*AH*XX*G*XXXXX*PHG, which is the consensus sequence proposed by Bairoch (31) for an iron binding domain (28). It has been suggested that the imidazole rings of the histidines coordinate the Fe^{2+} ion (31). Direct evidence for the role of iron in enzymatic activity comes from Kessler *et al.* (14), who showed that the ADH, ALDH, and pyruvate formate-lyase activities of the *E. coli* adhE enzyme were stimulated by iron. However, in a recent study of the *Giardia* EhADH2 homologue, Sanchez (9) reported that its ADH and ALDH activities were not dependent on iron or other metal ions for activity. We were able to demonstrate that the three conserved histidines located in the putative iron-binding domain of the EhADH2 enzyme are required for both its ADH and ALDH activity. This is consistent with the finding that both the ADH and ALDH activity of the EhADH2 enzyme require the presence of iron (2).

A histidine residue serves as a proton donor at the active site of zinc-dependent ADH molecules. Studies of the iron-dependent enzyme ADH(II) of *Z. mobilis* have shown that the histidine in position 277 (YNLPH^{277}GV), which is 10 amino acids removed from the terminal histidine within the putative iron-binding domain, appears to serve a similar function in *Z. mobilis* ADH(II) (23). The EhADH2 enzyme has a histidine at position 754 that is within the peptide VLLPH^{754}VI; this histidine is also 10 residues removed from the terminal histidine within the putative iron-binding domain (2). We found that the conservative replacement in EhADH2 of histidine 754 eliminates EhADH2 enzymatic activity. These data suggest that the catalytic mechanism of the ADH domain of EhADH2 may be similar to other members of the class III microbial enzymes. Although the inactivation of the ADH activity of EhADH2 by replacement of His^{754} was not unexpected, the finding that the site-directed mutagenesis of a single histidine in the putative active site of the ADH domain also completely eliminates ALDH enzymatic activity is surprising. Thus, our current findings suggest that the ALDH activity of EhADH2 is dependent on both a structurally intact C terminus and a functional ADH domain. Further studies will be necessary to determine whether this is because the ALDH activity of EhADH2 requires residues in the C terminus for substrate binding, catalysis, co-factor binding, or to maintain its appropriate conformation.

Studies of EhADH2 and the *E. coli* AdhE enzyme indicate that the minimal functional unit of the enzyme is a dimer and that both enzymes are capable of assembling dimers into helical structures called spirosomes, containing 20 or more dimers (2, 5, 8, 14). As noted above, we found that the recombinant EhADH2 molecule could form spirosomes, as did the mutant EhADH2(H754R), which lacks both ADH and ALDH activity.

[2] J. Hempel (University of Pittsburgh), personal communication.

Expression of EhADH2 in the *adhE* deletion *E. coli* strain SHH31 rescues its ability to grow in minimal media under anaerobic conditions. We found that co-expression of EhADH2 and EhADH2(H754R) in SHH31 led to spirosome production but did not rescue the ability of SHH31 to grow under anaerobic conditions. These data suggest that EhADH2(H754R) may serve as a dominant negative mutant by forming nonfunctional dimers with the EhADH2 enzyme. This could represent a potential approach for inhibiting the native *E. histolytica* enzyme as well. An alternative explanation for our findings would be a recombination event between the pEhADH2 and pEhADH2-(H754R) plasmids resulting in loss of the functional EhADH2 enzyme gene in doubly transformed SHH31. However, curing SHH31 of only the pEhADH2(H754R) plasmid restored the ability of SHH31 to grow under anaerobic conditions, indicating that an intact pEhADH2 plasmid was still present. Unfortunately, our inability to successfully express a mutant EhADH2 with an epitope tag that was capable of forming spirosomes[3] precluded the demonstration of heterodimer formation in these experiments.

In summary, the EhADH2 enzyme is required for *E. histolytica* growth and survival. Structural studies suggest that the C-terminal ADH domain of the enzyme functions as a separate entity, with a catalytic mechanism that may be similar to that seen in other class III microbial enzymes. However, the second component of the EhADH2, the N-terminal ALDH region, appears to be dependent upon an intact C terminus and intact ADH activity for ALDH enzyme activity. Further studies will be necessary to determine whether this dependence reflects conformational requirements or the evolutionary migration of substrate binding, co-factor binding, or catalytic sites from the N-terminal ALDH domain to the C terminus of EhADH2.

Acknowledgments—We thank Linda Kurz and John Hempel for many helpful discussions.

[3] A. Espinosa, L. Yan, Z. Zhang, L. Foster, D. Clark, E. Li, and S. L. Stanley, Jr., unpublished results.

REFERENCES

1. Lo, H.-S., and Reeves, R. E. (1978) *Biochem. J.* **171,** 225–230
2. Yang, W., Li, E., Kairong, T., and Stanley, S. L., Jr. (1994) *Mol. Biochem. Parasitol.* **64,** 253–260
3. Kumar, A., Shen, P.-S., Descoteaux, S., Pohl, J., Bailey, G., and Samuelson, J. (1992) *Proc. Natl. Acad. Sci. U. S. A.* **89,** 10188–10192
4. Rodriguez, M. A., Baez-Camargo, M., Delgadillo, D. M., and Orozco, E. (1996) *Biochim. Biophys. Acta* **1306,** 23–26
5. Bruchhaus, I., and Tannich, E. (1994) *Biochem. J.* **303,** 743–748
6. Zhang, W.-W., Shen, P.-S., Descoteaux, S., and Samuelson, J. (1994) *Mol. Biochem. Parasitol.* **63,** 157–161
7. Rosenthal, B., Mai, Z. M., Caplivski, D., Ghosh, S., De la Vega, H., Graf, T., and Samuelson, J. (1997) *J. Bacteriol.* **179,** 3736–3745
8. Goodlove, P. E., Cunningham, P. R., Parker, J., and Clark, D. P. (1989) *Gene* **85,** 209–214
9. Sanchez, L. B. (1998) *Arch Biochem. Biophys* **354,** 57–64
10. Fischer, R. J., Helms, J., and Durre, P. (1993) *J. Bacteriol.* **175,** 6959–6969
11. Nair, R. V., Bennett, G. N., and Papoutsakis, E. T. (1994) *J. Bacteriol.* **176,** 871–885
12. Arnau, J., Jorgensen, F., Madsen, S. M., Vrang, A., and Israelsen, H. (1998) *J. Bacteriol.* **180,** 3049–3055
13. Danielsson, O., Atrian, S., Luque, T., Hjelmqvist, L., Gonzàlez-Duarte, R., and Jörnvall, H. (1994) *Proc. Natl. Acad. Sci. U. S. A.* **91,** 4980–4984
14. Kessler, D., Leibrecht, I., and Knappe, J. (1991) *FEBS Lett.* **281,** 59–63
15. Matayoshi, S., Oda, H., and Sarwar, G. (1989) *J. Gen. Microbiol.* **135,** 525–529
16. Yong, T.-S., Li, E., Clark, D., and Stanley, S. L., Jr. (1996) *Proc. Natl. Acad. Sci. U. S. A.* **93,** 6464–6469
17. Ankri, S., Stolarsky, T., and Mirelman, D. (1998) *Mol. Microbiol.* **28,** 777–785
18. Hamann, L., Buss, H., and Tannich, E. (1997) *Mol. Biochem. Parasitol.* **84,** 83–91
19. Wang, W., and Malcolm, B. A. (1999) *BioTechniques* **26,** 680–682
20. Samuelson, J. (1999) *Antimicrob. Agents Chemother.* **43,** 1533–1541
21. Liu, Z. J., Sun, Y. J., Rose, J., Chung, Y. J., Hsiao, C. D., Chang, W. R., Kuo, I., Perozich, J., Lindahl, R., Hempel, J., and Wang, B. C. (1997) *Nat. Struct. Biol.* **4,** 317–326
22. Perozich, J., Nicholas, H., Wang, B., Lindahl, R., and Hempel, J. (1999) *Protein Sci.* **8,** 137–146
23. Cabiscol, E., Aguilar, J., and Ros, J. (1994) *J. Biol. Chem.* **269,** 6592–6597
24. Reeves, R. E. (1984) *Adv. Parasitol.* **23,** 105–142
25. Bracha, R., Nuchamowitz, Y., Leippe, M., and Mirelman, D. (1999) *Mol. Microbiol.* **34,** 463–472
26. Ankri, S., Padilla-Vaca, F., Stolarsky, T., Koole, L., Katz, U., and Mirelman, D. (1999) *Mol. Microbiol.* **33,** 327–337
27. Conway, T., Sewell, G. W., Osman, Y. A., and Ingram, L. O. (1987) *J. Bacteriol.* **169,** 2591–2597
28. Reid, M. F., and Fewson, C. A. (1994) *Crit. Rev. Microbiol.* **20,** 13–56
29. Guagliardi, A., Martino, M., Iaccarino, I., De Rosa, M., Rossi, M., and Bartolucci, S. (1996) *Int. J. Biochem. Cell Biol.* **28,** 239–246
30. Branden, C., and Tooze, J. (1991) *Introduction to Protein Structure*, Garland Publishing, Inc., New York
31. Bairoch, A. (1991) *Nucleic Acids Res.* **19,** 2241–2245